

# First-Principles Study on Electronic Properties, Phase Stability and Strain Properties of Cubic (Pm3m) and Tetragonal (P4mm) ATiO<sub>3</sub> (A=Pb, Sn)

N. N. Alam<sup>1,5</sup>, N. A. Malik<sup>1,5</sup>, N. H. Hussin<sup>2</sup>, A. M. M. Ali<sup>1,5</sup>, O. H. Hassan<sup>3,5</sup>, M. Z. A. Yahya<sup>4,5</sup> and M. F. M. Taib<sup>1,5\*</sup>

<sup>1</sup>Faculty of Applied Sciences, Universiti Teknologi MARA (UiTM), 40450 Shah Alam, Selangor, Malaysia.

<sup>2</sup>Faculty of Applied Sciences, Universiti Teknologi MARA (UiTM), 26400 Jengka, Pahang, Malaysia.

<sup>3</sup>Faculty of Arts and Design, Universiti Teknologi MARA, 40450 Shah Alam, Selangor, Malaysia.

<sup>4</sup>Faculty of Defence Science & Technology, Universiti Pertahanan Nasional Malaysia, 57100 Kuala Lumpur, Malaysia.

<sup>5</sup>Ionic Materials and Devices (iMADE), Institute of Science, Universiti Teknologi MARA, 40450 Shah Alam, Selangor, Malaysia.

## ABSTRACT

The electronic, phase stability and epitaxial strain properties of cubic and tetragonal structure of PbTiO<sub>3</sub> and SnTiO<sub>3</sub> were investigated using density functional theory (DFT) with space group (Pm3m) for cubic and (P4mm) for tetragonal for both structure within the GGA PBE-sol functional and were applied in a pseudo-potential plane wave using the CASTEP computer code. The results showed that the cubic PbTiO<sub>3</sub> and cubic SnTiO<sub>3</sub> have the minimum total energy within almost the tetragonal perovskite structure of the lattice parameter 3.937 Å and 3.916 Å respectively. The calculated electronic structure of SnTiO<sub>3</sub> resembles that of PbTiO<sub>3</sub> due to the Ti-3d states, Sn-5s and 5p states hybridize with the O-2p orbitals. The electronic properties showed that hybridizations happen among anion O 2p, special lone pair of ns<sub>2</sub>, and the Ti-3d states with an indirect bandgap at the X-G point. The energy band gap was evaluated from the division between the Ti-3d which the conduction band is and the upper of the O-2p valence band. It is achieved that the bond between Pb and O is ionic in the tetragonal state, while there is huge strength hybridization between Ti-3d and O-2p, which is significant for ferroelectricity in PbTiO<sub>3</sub>. It is shown that tetragonal is the steadiest when compared to other structures while the ilmenite structure is the least stable followed by a cubic, rhombohedral and orthorhombic. The out-of-plane c-axis strain is achieved to be largely oriented to PbTiO<sub>3</sub> under large in-plane a-axis compressive strain.

**Keywords:** Density Functional Theory, Electronic Properties, Phase Stability, Strain Properties

## 1. INTRODUCTION

Lead (II) titanate, PbTiO<sub>3</sub> is of great importance for electronic devices such as non-volatile memories, actuation devices and infrared sensors according to its piezoelectric and dielectric properties [1-2]. It also can be used as an optical sensor because it has a huge electro-optic coefficient and high photorefractive sensitivity [3-4]. PbTiO<sub>3</sub> which belongs to the P4mm group phase is in tetragonal symmetry and ferroelectric state in its low-temperature phase. PbTiO<sub>3</sub> experiences a transformation to a cubic and paraelectric state having symmetry group Pm3m at Curie temperature, T<sub>c</sub>=763 K [5]. Therefore, it is important to simulate both paraelectric and ferroelectric phases as there are two possibilities of phases existed for ATiO<sub>3</sub> (A=Pb, Sn) material. Unfortunately, in terms of public awareness, the toxicity of lead-based piezoelectrics is over impress, driving to possibly redundant social limit [6]. Modification to diminish the utilization of

\*Corresponding Author: mfariz@uitm.edu.my

harmful  $\text{Pb}^{2+}$ , for example, by replacement or doping procedures is essential. A look for replacement independent lead substance acquires property reaction of similar or even higher enormity triggers the necessity to evade the insertion of a poison element, which is lead, into next-batch electroactive materials [7].

$\text{SnTiO}_3$  is one of the promising lead-free ferroelectric materials, which is hypothetically having a high dielectric constant ( $\epsilon = 7.12$ ) and ferroelectric polarization ( $1.1 \text{ Cm}^{-2}$ ) [8].  $\text{Sn}^{2+}$  is generally used to structure a novel piezoelectric of free Pb-based material utilizing the first-principles study. Tin (II), Sn is expected to be a good replacement for lead since it is isoelectronic of lead [9]. Since the origination of the Bronze Age, Sn metal is environmentally friendly and has been broadly applied for tableware in the build of pewter alloys. Several latest computational researchers have proposed that replacing  $\text{A} = \text{Sn}^{2+}$  for  $\text{Pb}^{2+}$  in a polar perovskite with tetragonal  $\text{P4mm}$ ,  $\text{ATiO}_3$  structure will affect in piezoelectric (PT) and ferroelectric characteristics comparable to, or exceeding those, of mass PT [10-12]. Be that as it may, the majority of the hypothetical reports as to the  $\text{SnTiO}_3$  materials are significant around their physical properties and high polarization impact in the ferroelectric stage [13]. In this research, we accomplished the first-principles study of the electronic properties, cohesive energy and the impact of crystal size and strain on  $\text{PbTiO}_3$  and  $\text{SnTiO}_3$  by using the first-principles study of DFT.

## 2. COMPUTATIONAL METHOD

This work implements the first-principles study of density functional theory (DFT) using Cambridge Serial Total Energy Package (CASTEP) computer code plane-wave pseudopotential (PWPP). PWPP is a first-principles energy code that uses norm-conserving pseudopotentials (PP) and ultrasoft pseudopotentials (US-PP) [6]. All calculations for cubic and tetragonal are performed by general gradient approximation (GGA) with Perdew–Burke–Ernzerhof (PBE) and PBEsol exchange-correlation with the absence of spin orbit interaction [14]. Cut-off energy is set at 380 eV, the Monkhorst-Pack plot is utilized to calculate the Brillouin area, and the k-point is set as  $4 \times 4 \times 4$  [15]. A total energy of  $1.0e^{-5}$  eV/atom, 0.03 eV/Å maximum force, 0.5GPa for pressure and 0.001 Å for displacement has been employed throughout the calculation [14].

## 3. RESULTS AND DISCUSSION

### 3.1 Electronic Properties of PTO and SnTO

Figure 1 and Figure 2 display the electronic band structure of  $\text{PbTiO}_3$  and  $\text{SnTiO}_3$  in the cubic and tetragonal structures along the high symmetry lines of the Brillouin zone. The crystalline field and the electrostatic interactions between O 2p orbitals influenced the splits of these band structures which also can be seen in the density of states (DOS). The energy scale is found to be in electronvolts (eV) and the upper of the valence band was put to zero. The indirect bandgap of cubic  $\text{PbTiO}_3$  is 1.69 eV and 1.164 eV for  $\text{SnTiO}_3$  is seen in the direction (X–G) between the upper of the valence band at point X and the lower part of the conduction band at point G. The valence band and the conduction band possess the O-2p and the Ti-3d orbitals. The contribution to ferroelectric instability producing spontaneous polarization from the density of states (DOS) in Figure 3 later that Sn-5s, Sn-5p and O-2p orbitals have overlap and there are substantial covalent bonds between Sn and O atoms.

As for tetragonal structure, it is shown  $\text{PbTiO}_3$  has an indirect bandgap of 1.703 eV at X–G direction. The upper part valence band due to hybridization along the polar c-direction is thrust down as examine in contrast to the cubic state. In the electronic band structure of tetragonal  $\text{SnTiO}_3$ , at the Fermi level, there is the top of the valence band which is governed by the O-2p at X point. In the meantime, it is shown in Figure 4 the conduction band for  $\text{SnTiO}_3$  happens at G

point, which is mainly governed by Ti-3d assorted Sn p-state. The computation of the electronic bandgap appears that tetragonal SnTiO<sub>3</sub> has an indirect bandgap of 1.016 eV at X-G point. According to Cohen, to form a soft mode induced to ferroelectric instability, hybridization is importantly needed. The hybridization of Ti-3d and O-2p bands in SnTiO<sub>3</sub> is the same as that in PbTiO<sub>3</sub> [16]. Besides, the hybridization of Sn-5s and O-2p bands in SnTiO<sub>3</sub> are more similar to Pb-6s and O-2p in PbTiO<sub>3</sub>. This closeness shows that Sn is approximately close to Pb properties, can effortlessly construct covalent bonds with oxygen and that it is attainable that SnTiO<sub>3</sub> has excellent ferroelectric achievement just like PbTiO<sub>3</sub>.

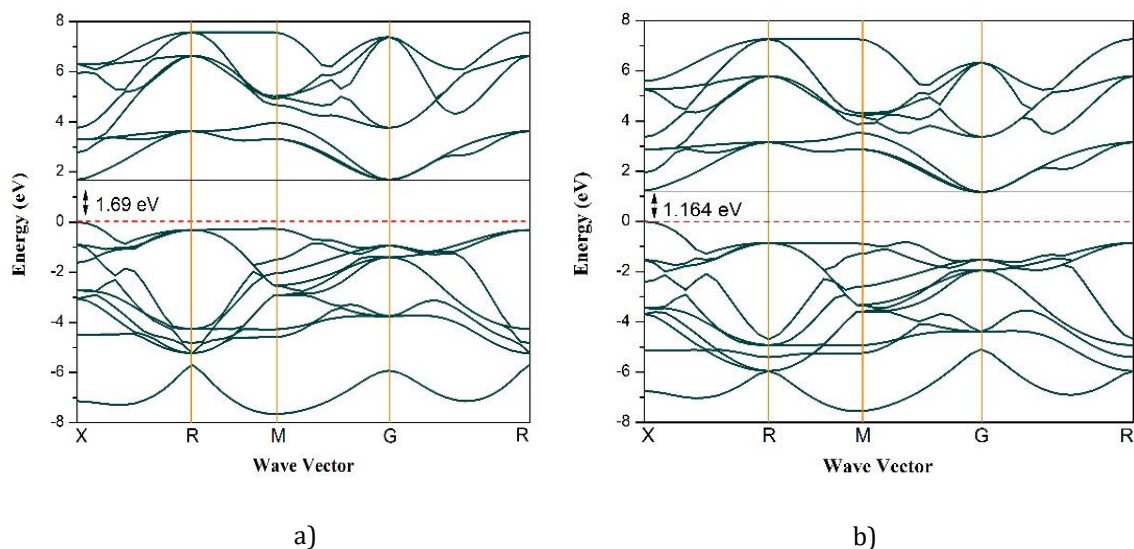


**Figure 1.** Calculated electronic bandgap of cubic a) PbTiO<sub>3</sub> and b) SnTiO<sub>3</sub>.

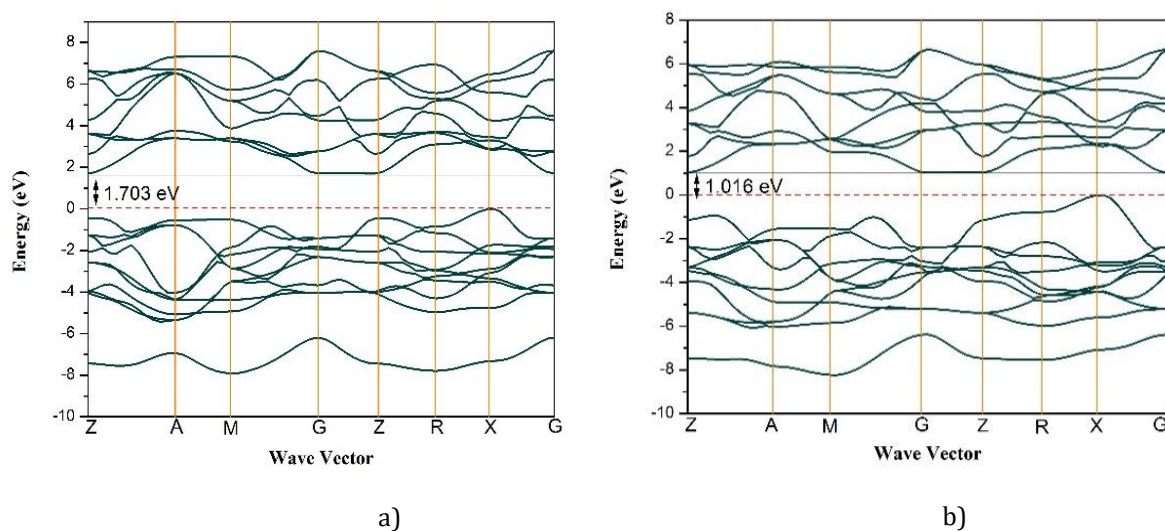


**Figure 2.** Calculated electronic bandgap of tetragonal a) PbTiO<sub>3</sub> and b) SnTiO<sub>3</sub>.

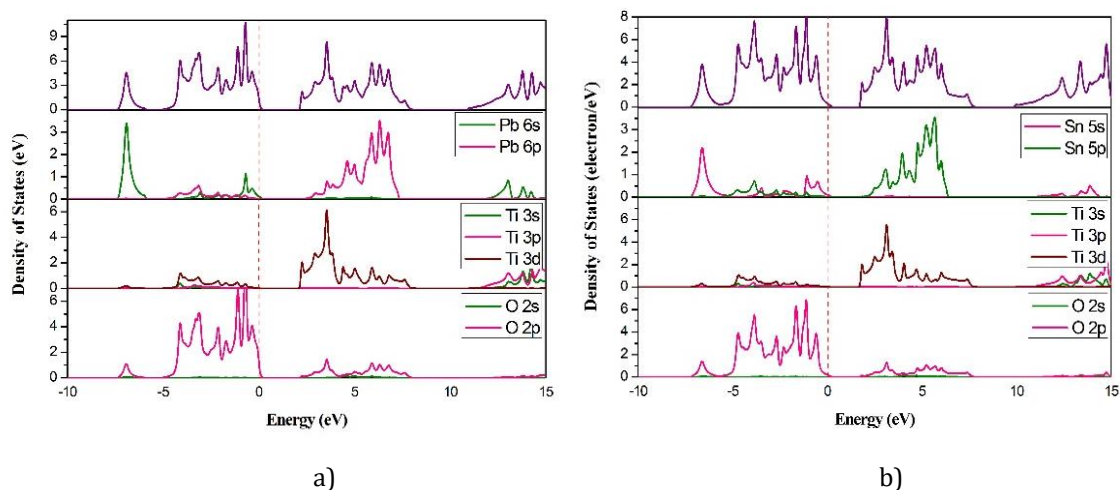


**Figure 3.** Calculated total density of states and partial density of states of cubic a)  $\text{PbTiO}_3$  and b)  $\text{SnTiO}_3$ .

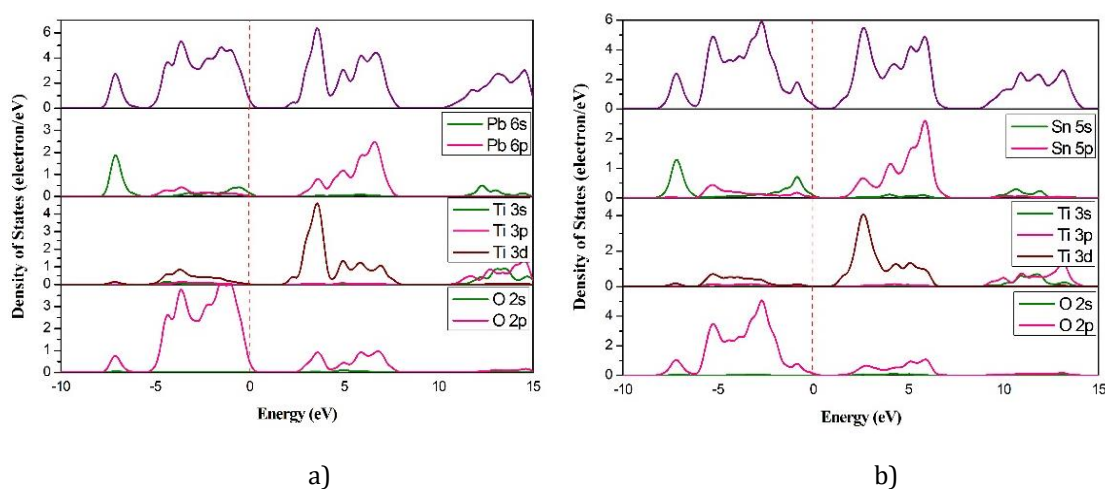


**Figure 4.** Calculated total density of states and partial density of states of tetragonal a)  $\text{PbTiO}_3$  and b)  $\text{SnTiO}_3$ .

### 3.1 Phase stability of Cubic and Tetragonal PTO and SnTO

The stability of a material can be assessed by figuring their improved structure and dissecting the firm vitality [17]. The cohesive energy of a material is the minimum energy required to break the solid into isolated atoms. Cohesive energy is significant because the energetic quality of a function can be tested and because of the range of densities tried, known as interminable and limited relating to the strong and nuclear frameworks, individually [18]. By utilizing the third-order Birch-Murnaghan equation, the mathematical representation for cohesive energy,  $E_{\text{coh}}$  is given by:

$$E_{\text{coh}} = E_{\text{tot}} - \sum_a^N E_a \quad (1)$$

Where  $E_a$  is the energy for each atom and  $N$  is the total number of atoms. Tetragonal demonstrate the least bend than other structures when GGA-PBESol functional is used, which indicates tetragonal is the steadiest structure at encompassing condition. The graph of the total energy value of the unit cell after volume enhancement is demonstrated in Figure 5. The outcome demonstrates for both graph  $\text{PbTiO}_3$  and  $\text{SnTiO}_3$  has the most minimal vitality at the polar structure with tetragonal  $P4mm$  with approximately  $-39$  eV contrasted with ilmenite with an

energy difference of almost 5 eV. This outcome is in great concurrence with most reports utilizing hypothetical and exploratory investigations by Hosseini et al [5] and Taib et al [19]. The determined energy is tabulated in Table 1.

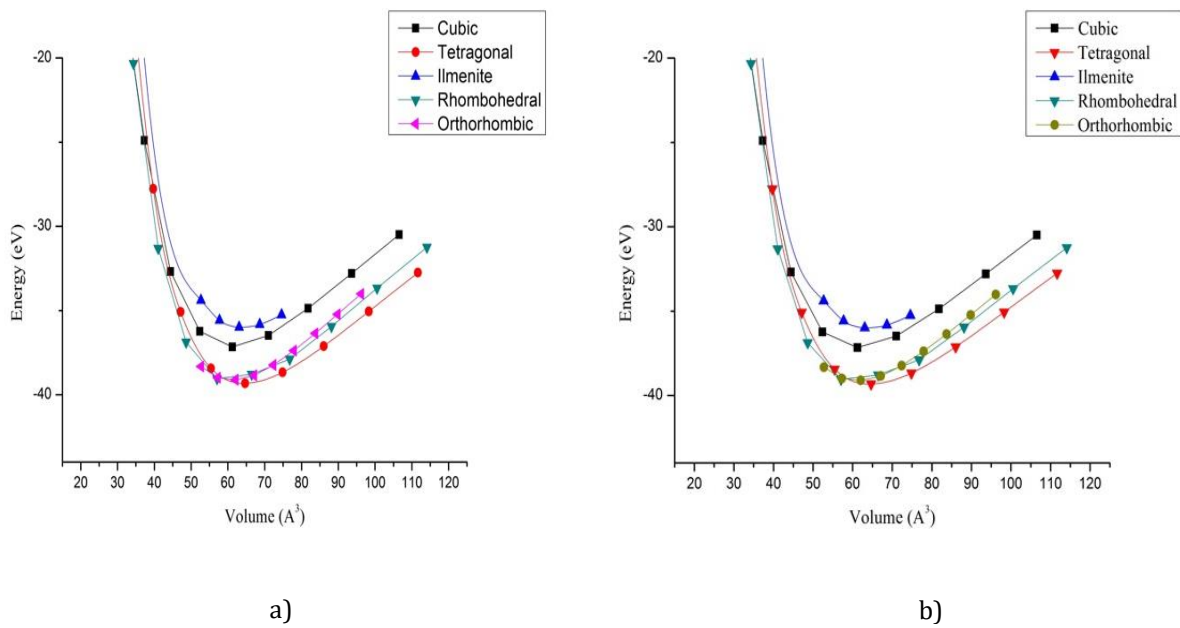


**Figure 5.** Phase stability of a)  $\text{PbTiO}_3$  and b)  $\text{SnTiO}_3$ .

**Table 1** Calculated Cohesive Energy (eV) for different phases of  $\text{ATiO}_3$  (A=Pb,Sn)

Compound	Space group	Crystal Name	Crystal Number	Cohesive Energy (eV)
<b><math>\text{PbTiO}_3</math></b>	Pm3m	Paraelectric Cubic	221	-37.153
	R3	Ilmenite	148	-34.383
	R3m	Rhombohedral	161	-38.779
	Pbam	Orthorhombic	62	-38.232
	P4mm	Tetragonal	99	-39.320
<b><math>\text{SnTiO}_3</math></b>	Pm3m	Paraelectric Cubic	221	-37.088
	R3	Ilmenite	148	-34.390
	R3m	Rhombohedral	161	-39.271
	Pbam	Orthorhombic	62	-38.310
	P4mm	Tetragonal	99	-39.523

### 3.2 Strain Properties of PTO and SnTO

The in-plane a-axis and out-of-plane c-axis misfit strains are evaluated based on the following equations [20][21]:

$$\epsilon_{\text{out-of-plane}} = \frac{c-a_0}{a_0} \times 100\% \quad (2)$$

$$\epsilon_{\text{in-plane}} = \frac{a-a_0}{a_0} \times 100\% \quad (3)$$



where  $a_0$  is the calculated lattice parameter for the cubic  $\text{PbTiO}_3$  and  $\text{SnTiO}_3$  ( $\text{Pm}3\text{m}$ ) phase. The value of  $a_0$  for  $\text{PbTiO}_3$  is 3.937 Å and 3.916 Å for  $\text{SnTiO}_3$ . The  $a$  is the lattice parameter of  $a$ -axis for tetragonal  $\text{PbTiO}_3$  and  $\text{SnTiO}_3$  ( $\text{P}4\text{mm}$ ) phase, and  $c$  is the lattice parameter of the  $c$ -axis for tetragonal  $\text{PbTiO}_3$  and  $\text{SnTiO}_3$  ( $\text{P}4\text{mm}$ ) phase. The volume impact such as tensile and compressive strain on material crystal structure is one of the most crucial basic studies on ferroelectric elements [22]. The evaluated total energy versus the out-of-plane strain lattice parameter  $c$  is demonstrated in Figure 6 and Figure 7 for  $\text{PbTiO}_3$  and  $\text{SnTiO}_3$  structure respectively. This work shows the in-plane  $a$ -axis compressive strain for  $\text{PbTiO}_3$  is constant at 3.861, 3.961, 4.061, 4.161, and 4.261 Å to symbolize the cubic.

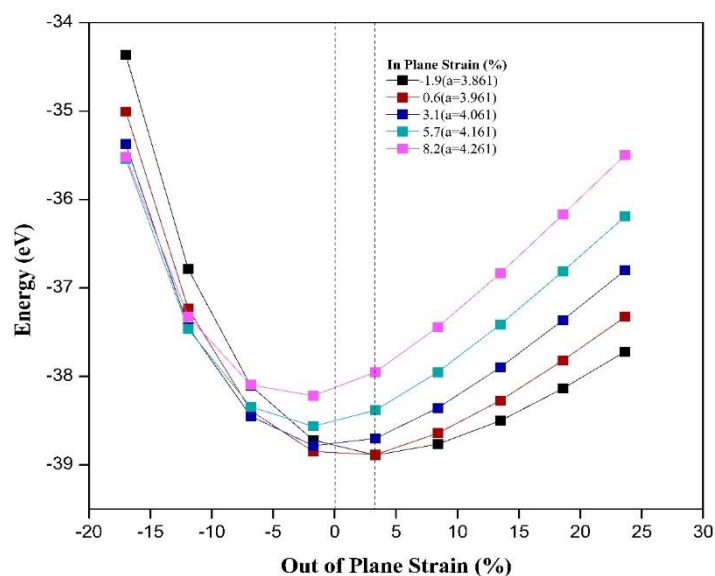


**Figure 6.** Computed energy of  $\text{PbTiO}_3$  relative to the out-of-plane  $c$ -axis tensile strain for different in-plane  $a$ -axis compressive strains.

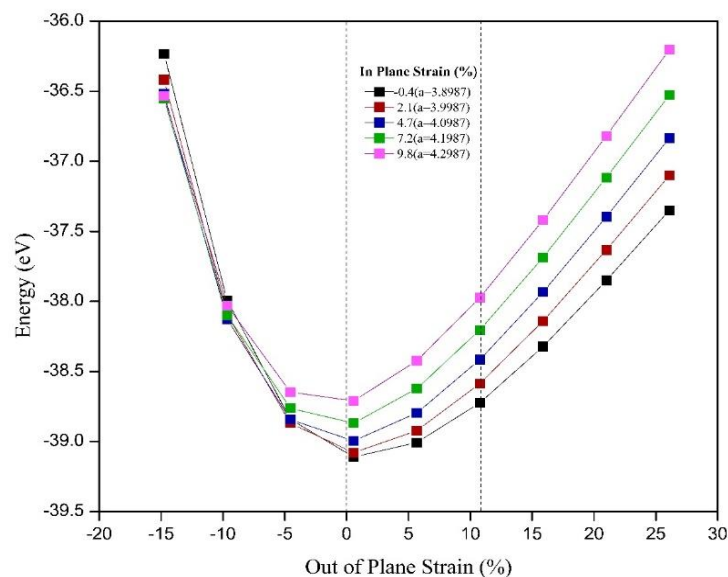


**Figure 7.** Computed energy of  $\text{SnTiO}_3$  relative to the out-of-plane  $c$ -axis tensile strain for different in-plane  $a$ -axis compressive strains.

The calculated cubic  $\text{PbTiO}_3$  and  $\text{SnTiO}_3$  lattice parameter of 3.973 Å and 3.941 Å respectively are used as  $a_0$  for the calculation of the in-plane and out-of-plane strain using the equations above. The in-plane  $a$ -axis compressive strain is pretend to be -1.9%, 0.6%, 3.1%, 5.7%, and 8.2% for

tetragonal  $\text{PbTiO}_3$  and -0.4%, 2.1%, 4.7%, 7.2%, and 9.8% for tetragonal  $\text{SnTiO}_3$ . The computed total energy proves that  $\text{PbTiO}_3$  is at the lowest energy under 3.1% of 4.061 Å of in-plane a-axis compressive strain for the lower out-of-plane strain lattice parameter c-axis (3.3%). Afterward,  $\text{SnTiO}_3$  is most stable under -0.4% of 3.899 Å for a smaller out-of-plane strain c-axis lattice parameter of 0.6%. At the same time,  $\text{PbTiO}_3$  is the most stable under more than -1.9% (3.861 Å) of in-plane a-axis compressive strain for greater out-of-plane c-axis tensile strain while for  $\text{SnTiO}_3$  it is most stable under bigger than -0.4% at a greater out-of-plane c-axis tensile strain.

#### 4. CONCLUSION

The band structure evaluation proved that the indirect energy bandgap of 1.69, 1.703, 1.164 and 1.016 eV respectively for cubic  $\text{PbTiO}_3$ , tetragonal  $\text{PbTiO}_3$ , cubic  $\text{SnTiO}_3$  and tetragonal phase  $\text{SnTiO}_3$  at the X-G direction. The DOS indicated that the upper valence states were governed by O-2p states while the conduction bands have components that are mainly constructed from the Ti d-state. Thus, these elements could be a great Pb-free element to be implemented in electro ceramic devices. DOS indicates the hybridization between lone pair ns<sup>2</sup> (n = 6, 5 for Pb, Sn respectively) and O-2p as well as the high strength covalence bonding Ti-O and A-O. Hybridization between an A-cation, such as Pb<sup>2+</sup>, can drive to the difference in the B-O relations which further stabilize the ferroelectric state, and polarizability of the B-cation is also advantageous to ferroelectricity. This work demonstrated that the ferroelectric perovskite structure of  $\text{PbTiO}_3$  and  $\text{SnTiO}_3$  with P4mm was unmistakably increasingly stable contrasted with the non-polar ilmenite structure. The evaluated total energy for strain effect shows that  $\text{PbTiO}_3$  is most stable or in the least energy state under 3.1% (4.061 Å) of in-plane a-axis compressive strain for the lower out-of-plane strain lattice parameter c-axis (3.3%) while  $\text{SnTiO}_3$  is most stable if the value is bigger than -0.4% at a greater out-of-plane c-axis tensile strain.

#### ACKNOWLEDGEMENTS

This work was supported by the Ministry of Higher Education (MOHE) Malaysia under FRGS grant 600-IRMI/FRGS 5/3 (337/2019) and University Technology MARA (UiTM) for the facilities provided.

#### REFERENCES

- [1] Zhang, S., Li, F., Jiang, X., Kim, J., Luo, J., & Geng, X. (2015). Advantages and challenges of relaxor- $\text{PbTiO}_3$  ferroelectric crystals for electroacoustic transducers - A review. *Progress in Materials Science*, 68, 1–66.
- [2] Bhatti, H. S., Hussain, S. T., Khan, F. A., & Hussain, S. (2016). Synthesis and induced multiferroicity of perovskite  $\text{PbTiO}_3$ ; A review. *Applied Surface Science*, 367, 291–306.
- [3] Essahlaoui, A., Essaoudi, H., Hallaoui, A., Bouhadda, M., Labzour, A., & Housni, A. (2018). Calculation of the thickness and optical constants of lead titanate thin films grown on MgO from their transmission spectra. *Journal of Materials and Environmental Science*, 9(1), 228–234.
- [4] Introduction, I. (2010). First-Principles Study of the Optical Properties of  $\text{PbTiO}_3$ . H. Salehi. 48(6), 829–843.
- [5] Hosseini, S., Movlaroo, T., & Kompany, A. (2007). First-principle calculations of the cohesive energy and the electronic properties of  $\text{PbTiO}_3$ . *Physica B: Condensed Matter*, 391(2), 316–321.
- [6] Kuma, S., & Woldemariam, M. M. (2019). Structural, Electronic, Lattice Dynamic, and Elastic Properties of  $\text{SnTiO}_3$  and  $\text{PbTiO}_3$  Using Density Functional Theory. *Advances in Condensed Matter Physics*, 2019.

- [7] Fan, Q., Biesold-McGee, G. V., Ma, J., Xu, Q., Pan, S., Peng, J., & Lin, Z. (2020). Lead-Free Halide Perovskite Nanocrystals: Crystal Structures, Synthesis, Stabilities, and Optical Properties. *Angewandte Chemie International Edition*, 59(3), 1030–1046.
- [8] Uratani, Y., Shishidou, T., & Oguchi, T. (2008). First-principles study of lead-free piezoelectric SnTiO<sub>3</sub>. *Japanese Journal of Applied Physics*, 47(9 PART 2), 7735–7739.
- [9] Pitike, K. C., Parker, W. D., Louis, L., & Nakhmanson, S. M. (2015). First-principles studies of lone-pair-induced distortions in epitaxial phases of perovskite SnTiO<sub>3</sub> and PbTiO<sub>3</sub>. *Physical Review B*, 91(3), 035112.
- [10] Pitike, K. C. (2018). Multiscale Modeling of Perovskite Ferroelectrics : From First Principles to Coarse-Grained Descriptions.
- [11] Gardner, J., Thakre, Atul., Kumar, Ashok., Scott, J. F. (2018). Tin Titanate – the hunt for a new ferroelectric perovskite.
- [12] Lyu, M., Yun, J. H., Chen, P., Hao, M., & Wang, L. (2017). Addressing Toxicity of Lead: Progress and Applications of Low-Toxic Metal Halide Perovskites and Their Derivatives. *Advanced Energy Materials*, 7(15).
- [13] Tarnaoui, M., Zaim, N., Kerouad, M., & Zaim, A. (2020). Elastic, electronic and electrocaloric properties near room temperature in Mn-doped SnTiO<sub>3</sub> from first-principles calculations. *Ceramics International*.
- [14] Hossain, M. K., Hossain, M. A., & Ahmed, F. (2020). First-Principles Study on Structural, Mechanical and Optoelectronic. *Solid State Communications*, 114024.
- [15] Taib, M., Yaakob, M., Badrudin, F., Kudin, T., Hassan, O., & Yahya, M. (2014). First Principles Calculation of Tetragonal (P4 mm) Pb-free Ferroelectric Oxide of SnTiO<sub>3</sub>. *Ferroelectrics*, 459(1), 134-142.
- [16] Inbar, I., & Cohen, R. (1996). Comparison of the electronic structures and energetics of ferroelectric and. *Physical Review B - Condensed Matter and Materials Physics*, 53(3), 1193–
- [17] Murnaghan, F.D., On the Theory of the Tension of an Elastic Cylinder. *Proceedings of the National Academy of Sciences*, 1944. 30(12): p. 382-384.
- [18] Hosseini, S. M., Movlarooy, T., & Kompany, A. (2007). First-principle calculations of the cohesive energy and the electronic properties of PbTiO<sub>3</sub>. *Physica B: Condensed Matter*, 391(2), 316–321.
- [19] Taib, M.F.M., et al., Structural, Electronic, and Lattice Dynamics of PbTiO<sub>3</sub>, SnTiO<sub>3</sub>, and SnZrO<sub>3</sub>: A Comparative First-Principles Study. *Integrated Ferroelectrics*, 2013. 142(1): p. 119-127.
- [20] Parker, W.D., J.M. Rondinelli, and S. Nakhmanson, First-principles study of misfit strain-stabilized ferroelectric SnTiO<sub>3</sub>. *Physical Review B*, 2011. 84(24): p. 245126.
- [21] Diéguez, O., K.M. Rabe, and D. Vanderbilt, First-principles study of epitaxial strain in perovskites. *Physical Review B*, 2005. 72(14): p. 144101.
- [22] Ederer, C. and N.A. Spaldin, Effect of epitaxial strain on the spontaneous polarization of thin film ferroelectrics. *Physical review letters*, 2005. 95(25): p. 257601.